

# Not All Instances Contribute Equally: Instance-adaptive Class Representation Learning for Few-Shot Visual Recognition

Mengya Han, Yibing Zhan, Yong Luo, Bo Du, Han Hu, Yonggang Wen *Fellow, IEEE*,  
and Dacheng Tao *Fellow, IEEE*

**Abstract**—Few-shot visual recognition refers to recognize novel visual concepts from a few labeled instances. Many few-shot visual recognition methods adopt the metric-based meta-learning paradigm by comparing the query representation with class representations to predict the category of query instance. However, current metric-based methods generally treat all instances equally and consequently often obtain biased class representation, considering not all instances are equally significant when summarizing the instance-level representations for the class-level representation. For example, some instances may contain unrepresentative information, such as too much background and information of unrelated concepts, which skew the results. To address the above issues, we propose a novel metric-based meta-learning framework termed instance-adaptive class representation learning network (ICRL-Net) for few-shot visual recognition. Specifically, we develop an adaptive instance revaluing network with the capability to address the biased representation issue when generating the class representation, by learning and assigning adaptive weights for different instances according to their relative significance in the support set of corresponding class. Additionally, we design an improved bilinear instance representation and incorporate two novel structural losses, i.e., intra-class instance clustering loss and inter-class representation distinguishing loss, to further regulate the instance revaluation process and refine the class representation. We conduct extensive experiments on four commonly adopted few-shot benchmarks: miniImageNet, tieredImageNet, CIFAR-FS, and FC100 datasets. The experimental results compared with the state-of-the-art approaches demonstrate the superiority of our ICRL-Net.

**Index Terms**—Few-shot, visual recognition, meta-learning, instance-adaptive, relative significance.

## I. INTRODUCTION

DEEP learning models have achieved the state-of-the-art performance on various visual tasks, including image classification [1]–[3], object detection [4], [5], and segmentation [6]. However, most deep models have numerous parameters and require large amounts of labeled data for training. In most cases, obtaining abundant labeled data is time-consuming

M. Han, Y. Luo and B. Du are with the National Engineering Research Center for Multimedia Software, School of Computer Science, Wuhan University, and Hubei LuoJia Laboratory, Wuhan, China (e-mail: myhan1996@whu.edu.cn; yluo180@gmail.com; dubo@whu.edu.cn). This work was done when Mengya Han was visiting JD Explore Academy as a research intern. Corresponding author: Yong Luo.

Y. Zhan and D. Tao are with JD.com (e-mail: zhanyibing@jd.com, dacheng.tao@gmail.com).

H. Hu is with the School of Information and Electronics, Beijing Institute of Technology, Beijing 100081, China (e-mail: hhu@bit.edu.cn).

Y. Wen is with the School of Computer Science and Engineering, Nanyang Technological University, Singapore 639798 (e-mail: ygwen@ntu.edu.sg).

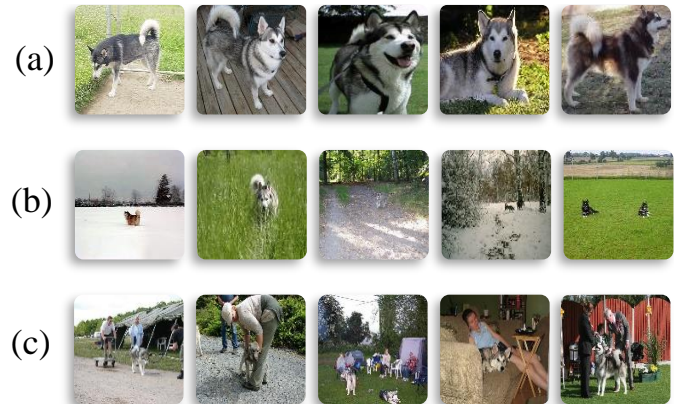


Fig. 1: Three types of support instances of one class: (a) shows representative support instances; (b) and (c) provide support instances that contain too much background and information of unrelated concepts, respectively. Intuitively, the more informative instances, such as the instances shown in row (a), will be more useful when obtaining class representations. Whereas, the instances in (b) and (c) should be revalued (often to be less important) in obtaining optimal class representation.

and laborious. The human annotation cost and data scarcity in some classes (e.g., rare species) significantly limit the applicability of current vision systems to learn new visual concepts efficiently. In contrast, learning from extremely few labeled instances is an important ability for humans. It is thus of great interest to develop machine learning algorithms that recognize new visual categories from only a limited amount of labeled instances for each novel category. The problem of learning to recognize unseen classes from limited instances, known as few-shot learning (FSL) [7], [8], has attracted increasing attention recently.

Few-shot visual recognition [9]–[17], as a specific FSL problem, attempts to learn a classifier with good generalization ability for novel visual concepts, each of which contains only a few labeled instances (support instances). To address this problem, a variety of solutions have been proposed. One mainstream solution is meta-learning [18]–[21], where a series of independent few-shot tasks are utilized to learn a general model during training, and then the general model is applied to unseen target tasks in the testing phase. In this way, the learned meta-models solve a new task by utilizing the knowledge acquired from many similar tasks. Generally, meta-learning methods for few-shot visual recognition can be classified into

two categories: optimization-based and metric-based. The former [22]–[24] automatically learns a set of model parameters, such as general initialization conditions, learning rates, and parameter updating strategies. The latter [25]–[27] aims to learn a discriminative embedding space, in which the representations of different instances and classes can be easily distinguished. Compared with optimization-based approaches, metric-based methods are more efficient and widely applicable, and thus we focus on metric-based ones in this paper.

In metric-based meta-learning methods for few-shot visual recognition, the instance representations are first extracted (such as by using neural networks). Then the class representations are obtained by utilizing the instances in the corresponding support set. Afterward, the query instances are classified by comparing the query representations with the obtained class representations. However, existing metric-based methods [28]–[30] often regard that all instances within the same support set are equally significant when obtaining the class-level representation. They ignore the information diversity that exists between the support instances and often obtain biased class representations, and hence sub-optimal performance can be achieved. For example, Fig. 1 provides three types of support instances of one class: (a) shows representative support instances, and (b) and (c) provide support instances that contain too much background and information of unrelated concepts (such as the person category) respectively. Intuitively, the more informative instances, such as the instances shown in Fig. 1 (a), will be more useful and should be revalued to be more important when obtaining the optimal class representation, while the instances in (b) and (c) should be revalued to contribute less.

This motivates our instance-adaptive class representation learning network (ICRL-Net), which adaptively revalues the importance of different instances in the same class when obtaining the class-level representation. The main contributions of this paper are:

- 1) We propose a novel metric-based meta-learning method, ICRL-Net, for few-shot visual recognition. Specifically, ICRL-Net contains an attentional bilinear feature extraction module that generates efficient instance-level representations, which can reduce the computational cost and improve the subsequent instance revaluation.
- 2) We develop an adaptive instance revaluing network to alleviate the issue of bias in class representation. Specifically, the adaptive instance revaluing network assigns different weights (or values) as the relative significance of instances by considering all support instances in the same classes and obtains the class representation by averaging the revalued instance representations.
- 3) We design a joint loss function to improve the instance adaptive revaluation process and refine the discriminative representation space of metric-based meta-learning. The designed joint loss function contains three components: a commonly adopted classification loss for few-shot visual recognition and two newly designed structural losses for robust representation: intra-class instance clustering loss and inter-class representation distinguishing loss.

We conducted extensive experiments on four popular few-shot benchmarks: miniImageNet [21], tieredImageNet [31], CIFAR-FS [32], and FC100 [33] datasets. The experimental results indicate that our ICRL-Net outperforms the state-of-the-art approaches. In specific, we achieved a significant 1.5% relative improvement compared with the most competitive counterpart. We further visualize the learned attention parts of ICRL-Net, and the results show that our ICRL-Net can appropriately identify the relative significance between instances in the same support set.

The rest of this paper is organized as follows. Section II briefly introduces the related works. The details of ICRL-Net are depicted in Section III. Section IV provides the experimental analysis, and we conclude this paper in Section V.

## II. RELATED WORK

This section briefly introduces the few-shot learning and the attention mechanism.

### A. Few-shot learning

Few-shot learning (FSL) is a emerging research topic that aims to learn a model from a set of data (base classes) and adapt the model to a disjoint set (new classes) with limited training data [34], [35]. Up to now, few-shot visual recognition [36]–[39], which aims to recognize novel visual categories from limited labeled instances, has received great attentions in FSL. Earlier work on few-shot learning tended to involve generative models with complex iterative inference strategies [8]. Most of the recent FSL approaches follow the meta-learning paradigm, which is usually performed by training a meta-learner that learns the transferable knowledge from similar tasks and then generalizes to new tasks. Under this paradigm, various meta-learning methods for few-shot learning are developed, and can be roughly classified into two categories: optimization-based methods and metric-based methods.

Optimization-based methods [20], [23], [24], [40]–[42] aim to find a single set of model parameters that can be adapted with a few steps of gradient descent to target tasks. For example, the well-known MAML approach [23] meta-learns a good initial condition (a set of neural network weights), which enables the model to quickly adapt to new tasks. The few-shot optimization approach Meta-LSTM [20] go further to not only learn a good initial condition but also an LSTM-based meta-learner that is utilized to learn appropriate parameter updating rules. Meta-SGD [40] further improves the meta-learning ability by learning the parameter initialization, gradient update direction, and learning rate within a single step. Although effective sometimes, using only a few instances to compute gradients in a high-dimensional parameter space could make generalization difficult. This issue is addressed by latent embedding optimization (LEO) [24], where a low-dimensional latent embedding of model parameters is learned and optimization-based meta-learning is performed in the embedding space. It turns out that the performance of meta-learning in low-dimensional parameter space is much better than that of meta-learning in high-dimensional space. Meta

transfer learning (MTL) [42] leverages the idea of transferring pre-trained weights and learns to effectively transfer large-scale pre-trained deep neural network weights for solving few-shot tasks. Overall, the approaches mentioned above still need to be fine-tuned on the target tasks. In contrast, metric-based methods solve target tasks without any model updates, thus avoid gradient computation during testing.

Metric-based methods [21], [29], [30], [33], [43]–[46] aim to learn a discriminative representation space, in which the distances between samples should be small in the same class, and large otherwise. The classification is performed in the space by simply finding the nearest neighbor of the query. For example, Koch et al. [44] calculate correlations between input instances via supervised metric based on siamese neural networks, and then predict the most relevant classes for query instances. Vinyals et al. [21] design a matching network that introduces an episodic training strategy for few-shot learning, and trains a neural network to embed examples. Additionally, an attention mechanism was used over the learned representations of the support set to predict the labels of the query set, which can be interpreted as a weighted nearest neighbor classifier. The popular prototypical network [29] is built upon [21], which takes a class’s prototype to be the mean of its support set in the representation space. Then, it calculates the distances between the class prototypes and the query representation to predict the category for a query instance. Inspired by semi-supervised clustering, Ren et al. [31] propose an extension of the prototypical network, which uses massive unlabeled instances to generate refined prototypes. These approaches focus on learning representations for data such that they can be recognized with a fixed metric [21], [29] or linear [29], [44] classifier. In the relation network [30], a deep distance metric is learned for comparing the relation between the query instances and the support instances. The metric is learnable and equivalent to a non-linear classifier. Cross attention network [47] is developed based on the relation network, where an attention module is designed to highlight the correct region of interest in query instance to help classification. Meta-Baseline [28] further improves the ability of metric-based methods by pre-training a classifier on all base classes and meta-learning on a nearest-centroid based few-shot classification algorithm. FEAT [48] takes advantage of the set-to-set function to generate task-adaptive feature representations. MCT [49] meta-learn the confidence for each query sample and then update class prototypes for each transduction step by using all the query examples with meta-learned scores. ReMP [50] proposes to refine the prototypes by considering the similarity information of the support set and query set to rectify the metric space, which aims to reduce the metric inconsistently between the training and testing phase. ICI [51], [52] assumes that not every unlabeled query instance is equal important and aims to exploit the unlabeled instances to augment the training set. It measures the credibility of pseudo-labeled examples and selects the most trustworthy pseudo-labeled samples according to their credibility as augmented labeled instances. However, most of the existing metric-based methods generally ignore the negative influence of support instances that contain too much interference information and often obtained biased class

representations [28], [29]. To address this issue, we propose a metric-based meta-learning method, ICRL-Net, which refines the class representation by revaluing the significance of different support instances based on the attention mechanism.

### B. Attention Mechanism

The attention mechanism can focus on the discriminative area adaptively and has been widely exploited for various tasks [3], [47], [53]. For example, Hu et al. [3] propose the squeeze-and-excitation network (SENet) to weight each channel of the feature map. Woo et al. [54] propose convolutional block attention module (CBAM), which employs hybrid spatial and channel features for attention design. These attention blocks either focus on the channel encoding or spatial context connection. In addition, there are other forms of attention mechanisms, such as graph attention [55] and self-attention [56], [57]. In few-shot learning, there are many works [21], [47], [48], [58], [59] also adopts the attention mechanism and achieved excellent performance. For example, in the matching network [21], attention mechanism is utilized together with the softmax function to fully specify the prediction of the meta-learner classifier. Similar to the matching network, the cross attention network [47] models the semantic dependency between support instances and query instances. Hence, the relevant regions on the query instances are adaptively localized so that the discrimination ability of embedding features can be improved. In general, matching network focuses on embeddings while cross attention network manipulates feature maps. FEAT [48] utilizes the self-attention [57] to generate task-adaptive feature representations. In contrast to these works, our developed AIRN mainly focus on learning robust class prototypes by identifying important support instances and suppressing irrelevant information.

## III. INSTANCE-ADAPTIVE CLASS REPRESENTATION LEARNING

This section depicts our Instance-adaptive Class Representation Learning Network (ICRL-Net).

### A. Problem Formulation

We first introduce the problem formulation of FSL. Let  $\mathcal{S}$  denote the support set, which contains  $N$  classes and  $K$  labeled instances per class. Then, given a query set  $\mathcal{Q}$ , FSL aims to determine the class of each unlabeled instance in  $\mathcal{Q}$  based on the support set  $\mathcal{S}$ . The setting mentioned above is also called the  $N$ -way  $K$ -shot classification task.

In FSL, the episodic training strategy [21] is often utilized to obtain a well-trained model by sampling few instances for every episode (an individual  $N$ -way  $K$ -shot task) under the meta-learning paradigm. We follow the episodic training strategy, which efficiently learns transferable knowledge from a relatively large labeled dataset  $\mathcal{D}_{train}$  that contains a set of classes  $\mathcal{C}_{train}$ . Then, the trained model is applied to a novel testing dataset  $\mathcal{D}_{test}$  that contains a set of classes  $\mathcal{C}_{test}$ . There are only a few labeled instances provided for each category in  $\mathcal{C}_{test}$ , and  $\mathcal{C}_{train} \cap \mathcal{C}_{test} = \emptyset$ . The process

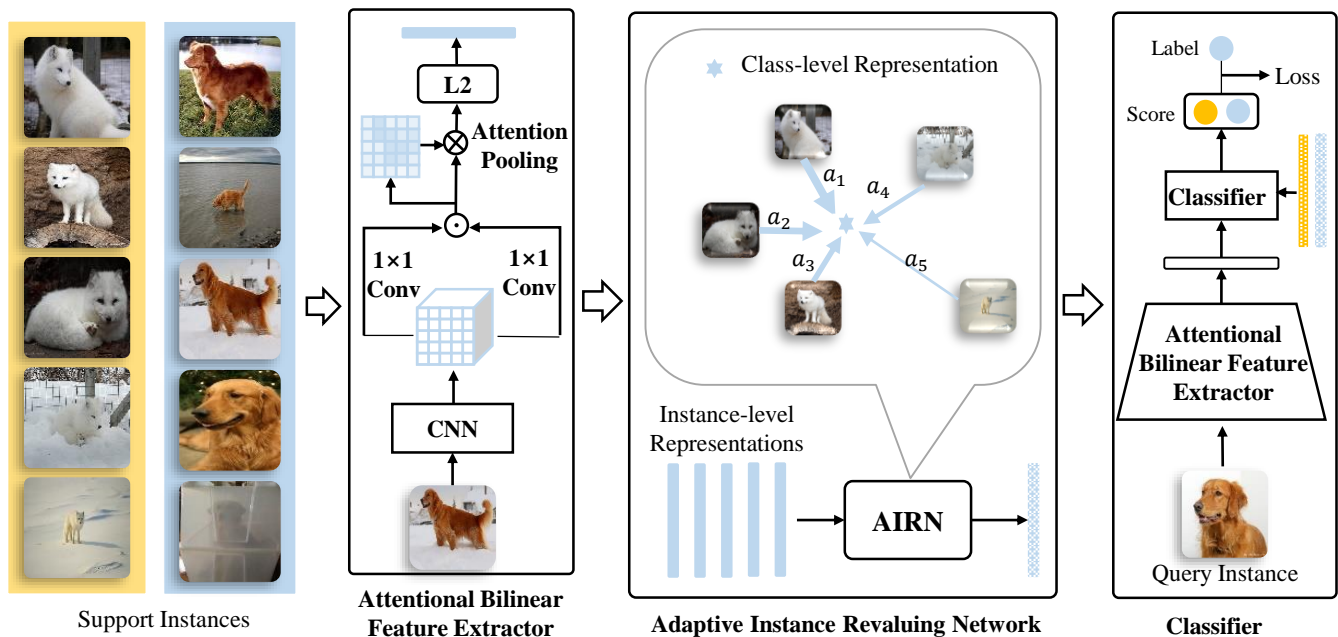


Fig. 2: Overview of the proposed ICRL-Net. ICRL-Net consists of an attentional bilinear feature extractor, an adaptive instance revaluing network, and a classifier. Specifically, ICRL-Net first extracts instance-level representations through the attentional bilinear feature extractor. Note that both support and query instances share the same feature extractor. Then, ICRL-Net uses the adaptive instance revaluing network to assign different values of support instances' relative significance and obtain the class-level representations from few-shot support instances. Finally, the query instances are classified by comparing the query instances' representations with the learned class representations of support instances.

of training is conducted on a series of episodes. In each episode, a small subset of  $N$  classes are sampled from  $\mathcal{C}_{train}$  to construct an  $N$ -way  $K$ -shot task: a support set  $\mathcal{S} = \{(x_n^k, y_n^k) | n = 1, \dots, N; k = 1, \dots, K\}$  and a query set  $\mathcal{Q} = \{(q_n^m, y_n^m) | n = 1, \dots, N; m = 1, \dots, M\}$ , where  $N$  is the number of classes in each episode,  $K$  is the number of support instances in each class, and  $M$  is the number of query instances in each class. In each episode, the model is trained by minimizing the prediction loss of the query set  $\mathcal{Q}$ .

In the testing, the generalization performances of the learned models are measured on the testing set episodes, each of which consists of a support set  $\mathcal{S}$  and a query set  $\mathcal{Q}$ , where  $\mathcal{S}$  and  $\mathcal{Q}$  are sampled from  $\mathcal{D}_{test}$  that contains classes distinct from those used in  $\mathcal{D}_{train}$ . The instance labels in the support set are known, while those in the query set are unknown and used only for evaluation. The predicted label of the query instance is given by taking the class that has the highest classification score.

## B. Overview

Fig. 2 presents the overview of our ICRL-Net. As shown in Fig. 2, ICRL-Net consists of three modules: an attentional bilinear feature extractor to extract instance-level representations, an adaptive instance revaluing network (AIRN) to learn the relative significance of support instances in the same class and accordingly obtains the class-level representations, and a classifier to classify each query instance based on the learned class-level representations. In addition, ICRL-Net is trained based on a designed joint loss, which contains a commonly adopted classification loss and two newly designed

structural losses: intra-class instance clustering loss and inter-class representation distinguishing loss. More details of the different components and losses are explained as follows.

## C. Attentional Bilinear Feature Extractor

Metric-based methods [21], [28], [29] perform classification by comparing the (support and query) instance representations, and thus it is critical to learn discriminative instance representation. It is well known that exploiting high-order information [60]–[62], such as by utilizing bilinear pooling, can improve the discriminative capability of feature representations compared with the low-order information [63]. Several few-shot works recently exploited a variety of variants of bilinear pooling to learn the better feature representation. For example, Second-order Similarity Network [64] leverages second-order pooling (i.e., Homogeneous Bilinear Pooling) to learn the second-order statistics for similarity learning. Following SoSN, Saliency-guided Hallucination Network [65], MsSoSN [66], and Few-shot Localizer [67] also employ second-order statistics to improve the accuracy which demonstrates the usefulness of second-order pooling in few-shot learning. The recent work [68] also gives a detailed theoretical analysis to demonstrate that the element-wise product of feature pairs can learn the correlations (higher-order statistics). Therefore, the element-wise product of the outputs of two  $1 \times 1$  convolutions can capture the higher-order statistics (correlations) for learning better feature representation. To learn a better instance-level feature representation and improve the revaluation process of AIRN, we propose an efficient feature extractor, namely, the attentional bilinear feature extractor.

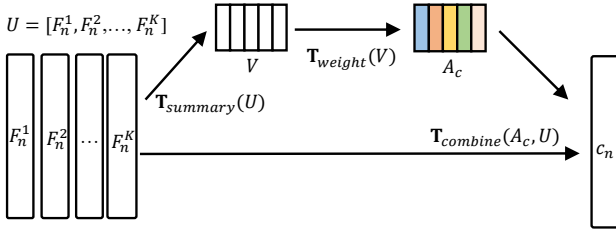


Fig. 3: The architecture of the adaptive instance revaluing network. It takes a set of instance-level representations as input, produces the relative significance of the corresponding instance, and then generates a class representation by weightedly combining them.

As shown in Fig. 2, our attentional bilinear feature extractor consists of a convolutional neural network followed by two parallel  $1 \times 1$  convolutional layers, an attention pooling, and an L2 normalization.

Specifically, given an input instance  $x_n^k$ , its initial feature representation is the output of a convolutional neural network given by  $f(x_n^k) \in \mathbb{R}^{d \times h \times w}$ , where  $d$ ,  $h$ , and  $w$  are the channel, height, and width number of the instance feature, respectively. Then two parallel convolutional layers with kernel size 1 are applied to each initial representation to generate two feature representations  $f_1 = f_{w_1}(f(x_n^k)) \in \mathbb{R}^{d \times h \times w}$  and  $f_2 = f_{w_2}(f(x_n^k)) \in \mathbb{R}^{d \times h \times w}$ , where  $w_1$  and  $w_2$  are parameters of two  $1 \times 1$  convolutional layers. Afterward, we compute the Hadamard product of two feature representations  $f_1$  and  $f_2$  to generate an intermediate feature representation  $f(x_n^k) = f_1 \odot f_2$ , where  $\odot$  denotes the element-wise multiplication. Attention pooling is applied on the intermediate representation  $f(x_n^k)$  for dimension reduction, where the spatial-wise weight  $A_s \in \mathbb{R}^{h \times w}$  for attention pooling is calculated as:

$$A_s = \delta(f_{w_s}(f(\hat{x}_n^k))), \quad (1)$$

where  $w_s$  denotes the parameter of a  $1 \times 1$  convolutional layer and  $\delta$  is the sigmoid function. Formally, the intermediate feature representation can be reshaped as  $f(\hat{x}_n^k) \in \mathbb{R}^{d \times hw}$ , and the spatial-wise attention weights can be reshaped as  $A_s \in \mathbb{R}^{hw \times 1}$ . Therefore, the final instance-level representation  $F_n^k \in \mathbb{R}^d$  of instance  $x_n^k$  is given by

$$F_n^k = L_2(f(\hat{x}_n^k) \cdot A_s). \quad (2)$$

where  $L_2$ -normalization is adopted. Both the query and support instances share the same feature extractor.

#### D. Adaptive Instance Revaluing Network

After learning the instance-level representation, one crucial problem of the metric-based paradigm for few-shot visual recognition is learning effective class-level representations from few support instance-level representations. Previous works treat all support instances equally when generating class-level representation [28], [29]. However, they ignore the instance diversity, and hence the resulting representation may be biased. For example, some support instances may contain too much background or unrelated concepts information. Therefore, when learning the class-level representation, different instances should have different contributions. In light

of the above analysis, we design an adaptive instance revaluing network (AIRN), which revalues the relative significance of all support instances in the same class. The class-level representation is obtained by adaptively and weightedly integrating instance-level representations according to their contributions. In this way, we can dynamically increase the importance value of more informative instances and decrease the weight of less informative instances.

The proposed architecture of AIRN is illustrated in Fig. 3. Specifically, given a support class  $n$  with  $K$ -shot instances, when  $K > 1$ , the union set of instance-level representations is denoted as

$$U = [F_n^1, \dots, F_n^K], \quad (3)$$

where each instance-level representation  $F_n^k = [r_1, \dots, r_d]$ ,  $d$  is the feature dimension and  $k \in \{1, \dots, K\}$ . Inspired by SENet [3], our we first calculate the ‘‘summary statistics’’ of each instance-level representation and outputs a statistical vector  $V = [v_1, \dots, v_K]$ , where each value  $v_k$  is calculated as follows,

$$v_i = \mathbf{T}_{summary}(F_n^k) = \frac{1}{d} \sum_{t=1}^d r_t, \quad (4)$$

Then we utilize two fully connected layers to learn the weight of each instance based on the statistical vector  $V$ . The set of instance weights  $A_c$  for class representation learning can be calculated as:

$$A_c = \mathbf{T}_{weight}(V) = \delta(w_4 \sigma(w_3 V)), \quad (5)$$

where  $A_c = [a_1, \dots, a_K]$  is a vector, and each value represents the relative significance of a corresponding instance,  $\delta$  denotes the sigmoid function,  $\sigma$  denotes the ReLU function, and  $w_3$  and  $w_4$  are the parameters of two fully connected layers.

Finally, the class-level representation of class  $n$  is given by:

$$c_n = \mathbf{T}_{combine}(A_c, U) = \sum_{k=1}^K a_k \cdot F_n^k, \quad (6)$$

where  $a_k$  is the relative significance of  $k$ -th instance.

#### E. Classifier

Following [28], we utilize the cosine classifier to classify query instances in the final classification stage. Specifically, given a query instance  $q_n^m$ , a classifier is followed by a softmax activation to generate a probability distribution, which is defined as

$$p(y = n | c_n, q_n^m) = \frac{\exp(w_n^T \cdot \hat{F}_n^m)}{\sum_{i=1}^N \exp(w_i^T \cdot \hat{F}_n^m)}, \quad (7)$$

and the predicted label of the query instance is

$$\hat{y} = \arg \max_{n \in \{1, \dots, N\}} (w_n^T \cdot \hat{F}_n^m), \quad (8)$$

where  $F_n^m$  is the instance-level representation of  $q_n^m$ , and  $w_n = \frac{c_n}{\|c_n\|_2}$  represents the weight parameter of class  $n$  in the cosine classifier.

### F. Optimization Loss

After predicting the labels of the instances in the query set  $\mathcal{Q}$ , we have the following classification loss on the query set:

$$L_{cls} = \sum_{(q_n^m, y_n^m \in \mathcal{Q})} \log(\hat{y} = y_n^m | q_n^m, \{c_n\}), \quad (9)$$

where  $L_{cls}$  is the cross-entropy loss,  $y_n^m$  and  $\hat{y}$  are the ground truth label and predicted label for the query instance  $q_n^m$ .

Meanwhile, in order to facilitate the learning of class-level representation, one solution is to decrease the similarities between the class-level representation of different classes and increase the similarities between the support instances and its own class-level representation. For example, [69] exploit the intra-class to inter-class variance-ratio to measure feature clustering and minimize the feature clustering loss to reduce intra-class variation among features during the training. This helps increase the inter-class distance and decrease the intra-class distance in the representation space, and enables the support instances to be more similar in the same class and dissimilar to other categories. Then the query instances can be easily classified. To achieve this goal, we design two novel structural losses, *i.e.*, intra-class instance clustering loss denoted as  $L_{intra}$  and inter-class representation distinguishing loss denoted as  $L_{inter}$ , to further refine the class-level representation, *i.e.*,

$$L_{intra} = \sum_{(x_n^k, y_n^k \in \mathcal{S})} \log(\hat{y} = y_n^k | x_n^k, \{c_n\}), \quad (10)$$

$$L_{inter} = \sum_{i \neq j} \hat{c}_i^T \hat{c}_j, \quad (11)$$

where  $\hat{c}_i = \frac{c_i}{\|c_i\|_2}$  and  $\hat{c}_j = \frac{c_j}{\|c_j\|_2}$ .

The overall objective function is a combination of  $L_{cls}$ ,  $L_{intra}$  and  $L_{inter}$ , *i.e.*,

$$L_{joint} = L_{cls} + \lambda_1 L_{intra} + \lambda_2 L_{inter}, \quad (12)$$

where  $\lambda_1$  and  $\lambda_2$  are trade-off hyper-parameters. The training procedure and the inference procedure of the ICRL-Net are summarized in Algorithm 1 and Algorithm 2, respectively.

## IV. EXPERIMENTS

To evaluate the effectiveness of the ICRL-Net, we conducted extensive experiments on four publicly available and widely used few-shot visual recognition benchmarks, *i.e.*, miniImageNet, tieredImageNet, CIFAR-FS, and FC100 datasets. In this section, we first introduce dataset details and experimental settings, and then comparisons with the state-of-the-art approaches. Finally, comprehensive ablation study is conducted to verify effectiveness of different components.

### A. Dataset

1) *MiniImageNet*: The miniImageNet dataset was initially proposed by [21], is a standard benchmark for few-shot visual recognition. MiniImageNet is a subset randomly sampled from the ImageNet [70] dataset. MiniImageNet includes a total number of 100 classes and 600 images per class. We follow

---

### Algorithm 1

The training process of ICRL-Net

---

**Input:** Training set  $\mathcal{D}_{train}$

```

1: while not done do
2:   Sample a  $N$ -way  $K$ -shot task  $(\mathcal{S}, \mathcal{Q})$  from  $\mathcal{D}_{train}$ 
3:   for  $n$  in  $1, \dots, N$  do
4:     for  $k$  in  $1, \dots, K$  do
5:       Generate  $F_n^k$  for support instance  $x_n^k$  using Eq. (2)
6:     end for
7:     Generate  $c_n$  for class  $n$  using Eq. (3)-Eq. (6)
8:   end for
9:   for  $n$  in  $1, \dots, N$  do
10:    for  $m$  in  $1, \dots, M$  do
11:      Generate  $F_n^m$  for instance  $q_n^m$  using Eq. (2)
12:      Predict  $\hat{y}$  for query instance  $q_n^m$  using Eq. (8)
13:    end for
14:  end for
15:  Compute the loss function  $L_{joint}$  using Eq. (12)
16:  Update the parameters of ICRL-Net with  $\nabla_{L_{joint}}$  using SGD
17: end while

```

---



---

### Algorithm 2

The inference process of ICRL-Net

---

**Input:** Testing set  $\mathcal{D}_{test}$

**Require:** The trained ICRL-Net

```

1: Sample a  $N$ -way  $K$ -shot task  $(\mathcal{S}, \mathcal{Q})$  from  $\mathcal{D}_{test}$ 
2: for  $n$  in  $1, \dots, N$  do
3:   for  $k$  in  $1, \dots, K$  do
4:     Generate  $F_n^k$  for support instance  $x_n^k$  using Eq. (2)
5:   end for
6:   Generate  $c_n$  for each class  $n$  using Eq. (3)-Eq. (6)
7: end for
8: for  $n$  in  $1, \dots, N$  do
9:   for  $m$  in  $1, \dots, M$  do
10:    Generate  $F_n^m$  for query instance  $q_n^m$  using Eq. (2)
11:    Predict  $\hat{y}$  for query instance  $q_n^m$  using Eq. (8)
12:   end for
13: end for
14: Compute the predict accuracy for each episode (task)

```

---

the split strategy proposed in [20] to split all 100 classes into three subsets. One subset that contains 64 classes is used for training. The other two subsets used for validation and testing include 16 and 20 classes, respectively. All images are resized to  $84 \times 84$ .

2) *TieredImageNet*: The tieredImageNet dataset was proposed by [31]. TieredImageNet is a relatively large subset sampled from ImageNet [70] dataset and consists of 608 classes that can be grouped into 34 high-level categories. The tieredImageNet dataset is split into three subsets: a training set, a validation set, and a testing set with 20, 6, and 8 high-level categories. The corresponding numbers of classes are 351, 97, and 160, respectively. All images are of size  $84 \times 84$ .

3) *CIFAR-FS*: The CIFAR-FS dataset [32] is a recently proposed few-shot visual recognition benchmark, consisting of all 100 classes from CIFAR-100 [71]. All images on these datasets are  $32 \times 32$ , and the number of images per class is

TABLE I: Comparisons with other state-of-the-art methods on miniImageNet and tieredImageNet. We use the officially provided results of all the other methods. The mean accuracy(%) of the proposed method ICRL-Net is obtained by over 600 testing episodes followed by the 95% confidence intervals(%). For each setting, the best result is highlighted. ‘-’ : not reported.

Model	Backbone	miniImageNet 5-way		tieredImageNet 5-way	
		1-shot	5-shot	1-shot	5-shot
Matching Networks [21]	ConvNet-4	43.56 ± 0.84	55.31 ± 0.73	-	-
Prototypical Networks [29]	ConvNet-4	49.42 ± 0.78	68.20 ± 0.66	53.31 ± 0.89	72.69 ± 0.74
MAML [23]	ConvNet-4	48.70 ± 1.84	63.10 ± 0.92	51.67 ± 1.81	70.30 ± 1.75
Relation Networks [30]	ConvNet-4	50.44 ± 0.82	65.32 ± 0.70	54.48 ± 0.93	71.32 ± 0.78
Das et.al [72]	ConvNet-4	52.68 ± 0.51	70.91 ± 0.85	-	-
wDAE-GNN [34]	WRN-28-10	62.96 ± 0.15	78.85 ± 0.10	68.18 ± 0.16	83.09 ± 0.12
LEO [24]	WRN-28-10	61.76 ± 0.08	77.59 ± 0.12	66.33 ± 0.05	81.44 ± 0.09
AWGIM [37]	WRN-28-10	63.12 ± 0.08	78.40 ± 0.11	67.69 ± 0.11	82.82 ± 0.13
PSST [36]	WRN-28-10	64.16 ± 0.44	80.64 ± 0.32	-	-
MTUNet [39]	WRN-28-10	56.12 ± 0.43	71.93 ± 0.40	62.42 ± 0.51	80.05 ± 0.46
MPM [11]	WRN-28-10	61.77	78.03	67.58	83.93
AFHN [38]	ResNet-18	62.38 ± 0.72	78.16 ± 0.56	-	-
VI-Net [25]	ResNet-18	61.05	78.60	-	-
TADAM [33]	ResNet-12	58.50 ± 0.30	76.70 ± 0.30	-	-
MTL [42]	ResNet-12	61.20 ± 1.80	75.50 ± 0.80	-	-
MetaOptNet [18]	ResNet-12	62.64 ± 0.61	78.63 ± 0.46	65.99 ± 0.72	81.56 ± 0.53
CAN [47]	ResNet-12	63.85 ± 0.48	79.44 ± 0.34	69.89 ± 0.51	84.23 ± 0.37
METANAS [22]	ResNet-12	61.70 ± 0.30	78.80 ± 0.20	-	-
DSN [26]	ResNet-12	62.64 ± 0.66	78.83 ± 0.45	66.22 ± 0.75	82.79 ± 0.48
RFS [27]	ResNet-12	62.02 ± 0.63	79.64 ± 0.44	69.74 ± 0.72	84.41 ± 0.55
SLA-AG [12]	ResNet-12	62.93 ± 0.63	79.63 ± 0.47	-	-
FEAT [48]	ResNet-12	<b>66.78</b>	82.05	70.80	84.79
DeepEMD [73]	ResNet12	65.9 ± 0.82	<b>82.41 ± 0.56</b>	<b>71.16 ± 0.87</b>	<b>86.03 ± 0.58</b>
MAN [13]	ResNet-12	61.70 ± 0.47	78.42 ± 0.34	65.99 ± 0.51	81.97 ± 0.37
ConstellationNet [59]	ResNet-12	64.89 ± 0.23	79.95 ± 0.17	-	-
Meta-UAFS [16]	ResNet-12	64.22 ± 0.67	79.99 ± 0.49	69.13 ± 0.84	84.33 ± 0.59
Meta-Baseline [28]	ResNet-12	63.17 ± 0.23	79.26 ± 0.17	68.62 ± 0.27	83.29 ± 0.18
Baseline	ResNet-12	62.71 ± 0.77	79.34 ± 0.56	68.30 ± 0.80	83.57 ± 0.63
ICRL-Net (OURS)	ResNet-12	65.55 ± 0.79	81.87 ± 0.51	70.56 ± 0.91	85.62 ± 0.64

TABLE II: A comparison of different methods on CIFAR-FS and FC100. We use the officially provided results of all the other methods. The mean accuracy(%) over 600 testing episodes is reported followed by the 95% confidence intervals(%). For each setting, the best result is highlighted. ‘-’ : not reported.

Model	Backbone	CIFAR-FS 5-way		FC100 5-way	
		1-shot	5-shot	1-shot	5-shot
MAML [21]	ConvNet-4	58.9 ± 1.9	71.5 ± 1.0	-	-
Prototypical Networks [29]	ConvNet-4	55.5 ± 0.7	72.0 ± 0.6	35.3 ± 0.6	48.6 ± 0.6
Relation Networks [30]	ConvNet-4	55.0 ± 1.0	69.3 ± 0.8	-	-
TADAM [33]	ResNet-12	-	-	40.1 ± 0.4	56.1 ± 0.4
MetaOptNet [18]	ResNet-12	72.0 ± 0.7	84.3 ± 0.5	41.1 ± 0.6	55.5 ± 0.6
DSN [26]	ResNet-12	72.3 ± 0.8	85.1 ± 0.6	-	-
SLA-AG [12]	ResNet-12	73.5 ± 0.7	86.7 ± 0.5	42.2 ± 0.6	59.2 ± 0.5
MABAS [74]	ResNet-12	73.5 ± 0.9	85.7 ± 0.6	42.3 ± 0.7	58.2 ± 0.7
ConstellationNet [59]	ResNet-12	75.4 ± 0.2	86.8 ± 0.2	43.8 ± 0.2	59.7 ± 0.2
Meta-UAFS [16]	ResNet-12	74.1 ± 0.7	85.9 ± 0.4	42.0 ± 0.6	57.4 ± 0.4
Baseline	ResNet-12	73.6 ± 0.6	85.4 ± 0.5	41.2 ± 0.6	57.1 ± 0.4
ICRL-Net (OURS)	ResNet-12	<b>75.8 ± 0.7</b>	<b>87.3 ± 0.5</b>	<b>44.5 ± 0.6</b>	<b>59.8 ± 0.6</b>

600. Following previous works [18], [26], we divide the whole dataset into 64, 16, and 20 classes for training, validation, and testing, respectively.

4) *FC100*: The FC100 dataset [33] is another benchmark derived from CIFAR-100 [71]. There are 60 classes from 12 different superclasses for training, 20 classes from 4 different superclasses for validation, and 20 classes from 4 different superclasses for testing. Similar to the CIFAR-FS dataset,

every class has 600 images of size  $32 \times 32$ .

### B. Implementation Details

1) *Pre-training Process*: Following the previous works [28], [48], we apply an additional pre-training phase to train the backbone network. Thus, the backbone network, appended with a linear layer, is trained to classify all training classes (e.g., 64 classes in the miniImageNet)

based on the cross-entropy loss. We follow the conventional deep learning pipeline and divide each training class into two parts: model training and validation. In this stage, the learning rate is set to 0.1. For all datasets, random resized crop and horizontal flip data augmentations are used for model optimization. The classification performance over features of sampled 1-shot tasks from the model validation split is evaluated to select the best pre-trained model, whose weights are then used to initialize the backbone network in the meta-training phase.

2) *Meta-training Process*: We follow the episodic training strategy [21] to train the ICRL-Net in the meta-training phase. Specifically, the pre-trained backbone network is finetuned at a learning rate of 0.001. Meanwhile, other parts of ICRL-Net are initialized randomly and optimized with a learning rate of 0.01. We set the total number of the training epoch to be 200, and each epoch contains 100 episodes. All experiments are implemented in PyTorch on an Ubuntu server with a single NVIDIA V100 GPU card. We adopt SGD with a Nesterov momentum of 0.9 and weight decay of 0.0005 for model optimization in both pre-training and meta-training. Moreover, the learning rate decay is set to 0.1 in two in both pre-training and meta-training. We adopt the same data augmentation (i.e., random horizontal flip and random resized crop) when dealing with all datasets during meta-training. More implementation details can be found in the supplementary material.

### C. Performance Comparison

We compared the proposed method with state-of-the-art methods, such as MAML [23], LEO [24], MTL [42], Matching Networks [21], Prototypical Networks [29], Relation Networks [30], CAN [47], Meta-Baseline [28], and DSN [26].

1) *Performance on miniImageNet and tieredImageNet*: Table I shows the performance of all comparison methods on miniImageNet and tieredImageNet. The best results are highlighted in boldface.

On the miniImageNet dataset, we observe that the proposed method ICRL-Net can achieve comparable performance compared with state-of-the-art methods under both 5-way 1-shot and 5-shot settings and achieves the accuracies with 65.55% and 81.87% on 1-shot and 5-shot, respectively. Compared with several state-of-the-art approaches, such as PSST [36], ConstellationNet [59], and Meta-Baseline [28]. We observe that the proposed ICRL-Net achieves the best performance compared to these state-of-the-art algorithms. Note that our baseline is the same as Meta-Baseline [28], and they have a similar performance. Compared to Meta-Baseline, ICRL-Net brings significant improvements and improves 1-shot accuracy by 2.38% and 5-shot accuracy by 2.61%. Moreover, our approach has such an improvement attributed to the adaptive instance revaluing strategy that facilitates learning optimal class representations. The improvements demonstrate that the necessity of considering the instance diversity for improving the class representation learning.

On the tieredImageNet dataset, it is worth noting that the principle of dividing the training set and testing set is according to the disjoint sets, where the similarity of classes

TABLE III: Ablation study of the AIRN.

Method	miniImageNet 5-shot	tieredImageNet 5-shot
Baseline	79.34 $\pm$ 0.56	83.57 $\pm$ 0.63
+ AIRN	80.63 $\pm$ 0.58	84.64 $\pm$ 0.57

TABLE IV: Ablation study of generating weights to aggregate  $K$ -shot instances.

Method	miniImageNet 5-shot	tieredImageNet 5-shot
Similarity-type	79.25 $\pm$ 0.54	84.02 $\pm$ 0.60
Attention-type	79.89 $\pm$ 0.56	84.27 $\pm$ 0.62
AIRN	80.63 $\pm$ 0.58	84.64 $\pm$ 0.57

in each disjoint set is relatively high. Thus, it is more difficult to distinguish the categories in the training set and testing set. Nevertheless, on the tieredImageNet dataset, we observe that the proposed ICRL-Net still achieves comparable performance compared to other state-of-the-art algorithms. For example, on tieredImageNet, the 5-way 1-shot and 5-shot accuracies of FEAT are 70.80% and 84.79%, respectively, and the accuracies of ICRL-Net are 70.56% and 85.62%, respectively. Note that our baseline is the same as Meta-Baseline [28], and they have a similar performance. Compared to Meta-Baseline [28], our ICRL-Net achieves a significant improvement of 1.94% and 2.33% accuracies for 1-shot classification and 5-shot classification, respectively. The improvements also prove the effectiveness of our approach.

2) *Performance on CIFAR-FS and FC100*: Experimental results on CIFAR-FS and FC100 are shown in Table II. The best results are highlighted in boldface. Our method also consistently outperforms the other state-of-the-art methods under both 1-shot and 5-shot settings on the CIFAR-FS and FC100 datasets. For the CIFAR-FS dataset, our method outperforms the sub-optimal method by 0.4% on 1-shot and 0.5% on 5-shot. Notice that our ICRL-Net perform much better than the methods based on the average class representation: MetaOptNet [18] and Meta-Baseline [28]. For the FC100 dataset, our method also improves the classification performance by 0.7% and 0.1% under 1-shot and 5-shot settings, respectively. The results show the necessity and effectiveness of learning an optimal class representation.

### D. Ablation Study

In this subsection, we conduct ablation studies to assess the effectiveness of each component of ICRL-Net, including AIRN, the attentional bilinear feature extractor, and the designed loss function. We refer to the supplementary material for more studies.

1) *Influence of the AIRN*: In our baseline, the class-level representation is generated by directly averaging a few support instance representations, and the performance is similar to Meta-Baseline [28]. Our ICRL-Net improves this baseline by designing the AIRN module, the attentional bilinear feature extractor, and novel loss function. To evaluate the effectiveness of the proposed AIRN, we directly add this module on the baseline. Table III reports the comparison results under the



TABLE V: A comparison of different variants of our bilinear feature extractor with the extractor based on naive bilinear pooling [62]. In ‘Model-1’, global average pooling (instead of attention pooling) is adopted in the feature extractor of our ICRL-Net; In ‘Model-2’, attention pooling is removed from our extractor; In ‘Model-3’, the two  $1 \times 1$  convolutional layers is removed from our extractor; ‘Model-4’ is to utilize only one  $1 \times 1$  convolutional layer to transform the features in our extractor; Finally, ‘Model-5’ is to utilize naive bilinear pooling [62] in the feature extractor.

Method	miniImageNet 5-way		tieredImageNet 5-way	
	1-shot	5-shot	1-shot	5-shot
Model-1	63.86 $\pm$ 0.80	81.23 $\pm$ 0.50	69.50 $\pm$ 0.82	84.94 $\pm$ 0.62
Model-2	64.86 $\pm$ 0.81	81.67 $\pm$ 0.54	70.13 $\pm$ 0.83	85.33 $\pm$ 0.66
Model-3	64.62 $\pm$ 0.84	81.56 $\pm$ 0.53	70.22 $\pm$ 0.84	85.10 $\pm$ 0.60
Model-4	64.30 $\pm$ 0.77	81.25 $\pm$ 0.52	69.86 $\pm$ 0.80	85.14 $\pm$ 0.63
Model-5	64.05 $\pm$ 0.76	80.78 $\pm$ 0.56	69.44 $\pm$ 0.86	84.76 $\pm$ 0.58
ICRL-Net	65.55 $\pm$ 0.79	81.87 $\pm$ 0.51	70.56 $\pm$ 0.91	85.62 $\pm$ 0.64

TABLE VI: The influence of the joint loss function. We compared the joint loss with other loss functions, including the original classification loss function  $L_{cls}$  (i.e., cross entropy loss), the  $L_{cls} + L_{inter}$  loss function, and the  $L_{cls} + L_{intra}$  loss function.

Loss Function	miniImageNet 5-way		tieredImageNet 5-way	
	1-shot	5-shot	1-shot	5-shot
$L_{cls}$	64.32 $\pm$ 0.80	81.12 $\pm$ 0.52	69.62 $\pm$ 0.84	85.07 $\pm$ 0.61
$L_{cls} + L_{inter}$	65.26 $\pm$ 0.78	81.43 $\pm$ 0.56	70.32 $\pm$ 0.91	85.38 $\pm$ 0.61
$L_{cls} + L_{intra}$	65.03 $\pm$ 0.80	81.50 $\pm$ 0.58	69.87 $\pm$ 0.84	85.24 $\pm$ 0.62
$L_{joint}$	65.55 $\pm$ 0.79	81.87 $\pm$ 0.51	70.56 $\pm$ 0.91	85.62 $\pm$ 0.64

1-shot and 5-shot settings. From the results, we observe that utilizing AIRN leads to significant improvements on 5-shot tasks compared with the baseline. These improvements verify our intuition that the relative importance of few-shot support instances in the same class should be different when learning class-level representations. For 1-shot tasks, since there is only one support instance per class. Therefore, class-level representation is just the instance-level representation, and AIRN does not take effect in 1-shot tasks.

To further demonstrate effectiveness of the proposed AIRN, we add some experiments that adopt other approaches to aggregate  $K$ -shot instances, such as similarity-type weights, attention-type weights. The experimental results are shown in Table IV. The AIRN module allows the model to pay more attention to the most informative support instance features while suppressing those unimportant support instance features, and has the best performance when learning class-level representations.

### 2) Influence of the Attention Bilinear Feature Extractor:

To verify the effectiveness of the attentional bilinear feature extractor, we develop various variants of ICRL-Net to perform the process from the instance features to instance-level representations. In ‘Model-1’, global average pooling (instead of attention pooling) is adopted in the feature extractor of our ICRL-Net; In ‘Model-2’, attention pooling is removed from our extractor; In ‘Model-3’, the two  $1 \times 1$  convolutional layers is re-moved from our extractor; ‘Model-4’ is to utilize only one  $1 \times 1$  convolutional layer to transform the features in our extractor; Finally, ‘Model-5’ is to utilize naive bilinear pooling [62] in the feature extractor. Table V shows the comparison results under 1-shot and 5-shot settings. The results indicate that the attentional bilinear feature extractor yields better results than other variants. Therefore, it can conclude that the attention bilinear strategy is conducive to learning a

discriminative and informative instance-level representation.

3) *Influence of the Joint Loss Functions:* To demonstrate the effectiveness of the designed loss function, we compare the joint loss with three loss functions, including the original classification loss function  $L_{cls}$ , the  $L_{cls} + L_{inter}$  loss function, and the  $L_{cls} + L_{intra}$  loss function. The results are shown in Table VI. Compared with other loss functions, the designed loss function achieves the highest accuracy in 5-way 1-shot and 5-way 5-shot tasks. Moreover, the accuracies of using the  $L_{cls} + L_{inter}$  and  $L_{cls} + L_{intra}$  are higher than the original classification loss function  $L_{cls}$ , indicating that the proposed loss function is efficient for the representation learning of FSL.

4) *Comparison on Different K-shot Settings:* To further demonstrate the effectiveness of the adaptive instance revaluation strategy, we compare ICRL-Net with the baseline method under more  $K$ -shot ( $K=1,3,5,7,10,20$ ) settings. The comparison results are shown in Fig. 4. From the results, we observe that ICRL-Net consistently outperforms the baseline under various  $K$ -shot settings on miniImageNet and tieredImageNet datasets. The improvements again demonstrate the ability of ICRL-Net and validate the necessity and effectiveness of revaluing the importance of support instances when obtaining the class-level representation.

5) *Hyper-parameter Analysis:* We also conduct sensitivity analysis for the two trade-off hyper-parameters in our joint loss. The experiments are performed by fixing the value of one hyper-parameter and then changing the value of another hyper-parameter. In specific, when analyzing hyper-parameter  $\lambda_1$ , the value of hyper-parameter  $\lambda_2$  is set to 0.1. Similarly, when analyzing hyper-parameter  $\lambda_2$ , the value of hyper-parameter  $\lambda_1$  is set to 0.1. The experimental results are shown in Fig. 5. We observe that the best performances are achieved when  $\lambda_1 = \lambda_2 = 0.1$ , and this setting is adopted in all experiments.

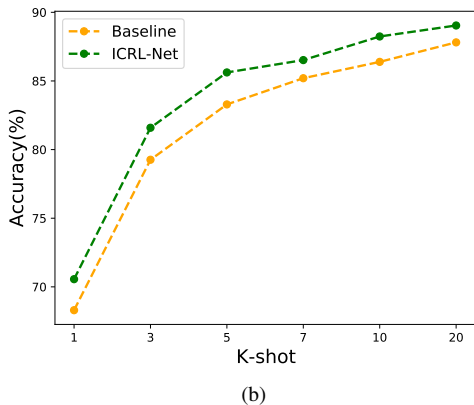
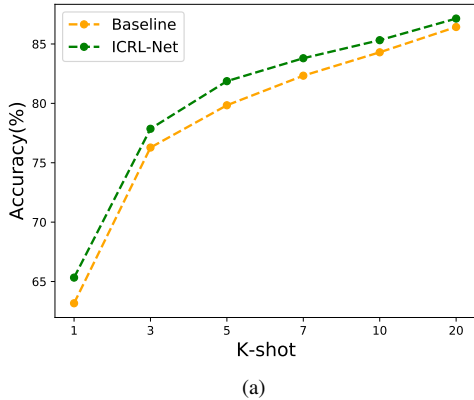


Fig. 4: The results w.r.t. different K-shot settings on miniImageNet and tieredImageNet. (a): 5-way classification on miniImageNet. (b): 5-way classification on tieredImageNet.

### E. Visualization of Relative Significance

We visualize the values of the relative significance of support instances to verify the effectiveness of the proposed method. We randomly selected several group examples from the miniImageNet and tieredImageNet, and each group contains five support instances from the same class. The visualization results of the relative importance are shown in Fig. 6. Each column (group) of support instances is sorted by relative importance. It shows that more informative instances are generally assigned with larger importance weights according to ICRL-Net, except the column (e). This might due to multiple instances contain information related to other concepts, and our method does not accurately express the actual concepts of the instances. Therefore, in the future, we will focus on correctly expressing the target information related to the category when the instance contains multiple targets. We also visualize the learned attention maps in the supplementary material.

### F. Cross-domain FSL

Beyond the standard single domain few-shot classification setting, we introduce a more challenging and realistic cross-domain setting. In this new setting, we aim to test the

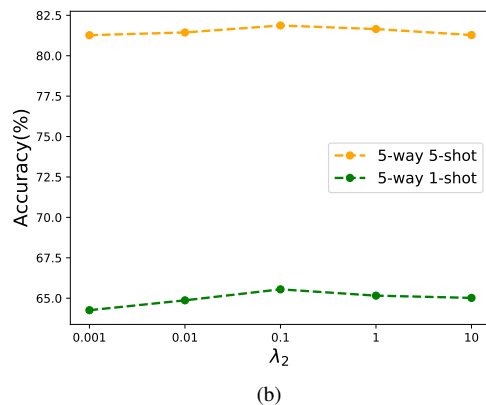
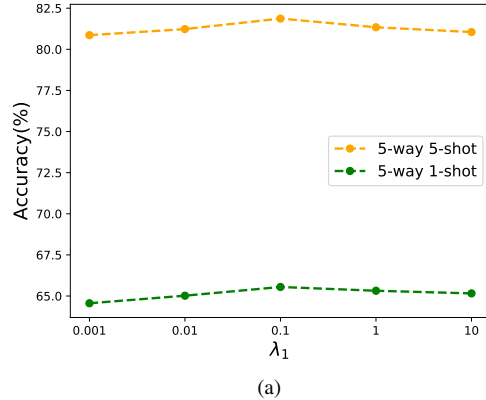


Fig. 5: The results of parameters analysis on miniImageNet.

TABLE VII: 5-shot classification accuracy under dataset shift.

Model (%)	miniImageNet $\rightarrow$ CUB
Linear Classifier [75]	65.57 $\pm$ 0.70
Cosine Classifier [75]	62.04 $\pm$ 0.76
MetaOptNet-SVM [18]	54.67 $\pm$ 0.56
Baseline	64.86 $\pm$ 0.73
<b>ICRL-Net</b>	<b>67.08 <math>\pm</math> 0.55</b>

generalization of a trained model across previously unseen domains (datasets) with different data distributions. Cross-domain few-shot learning can better evaluate the model's generalization ability to novel tasks. Following the instructions of [75], we conducted a cross-domain few-shot experiment by training the models on the miniImageNet training set and evaluating the model on the CUB200 testing set. This set of experiments is designed to evaluate the performance of different algorithms when the distribution divergence between training and testing sets is large. To fairly compare with other approaches, we adopt the CUB testing split presented in their original work. The comparison results are reported in Table VII, where we can see that the proposed ICRL-Net can outperform other approaches. The cross-domain few-shot settings further demonstrate the effectiveness of the proposed method.

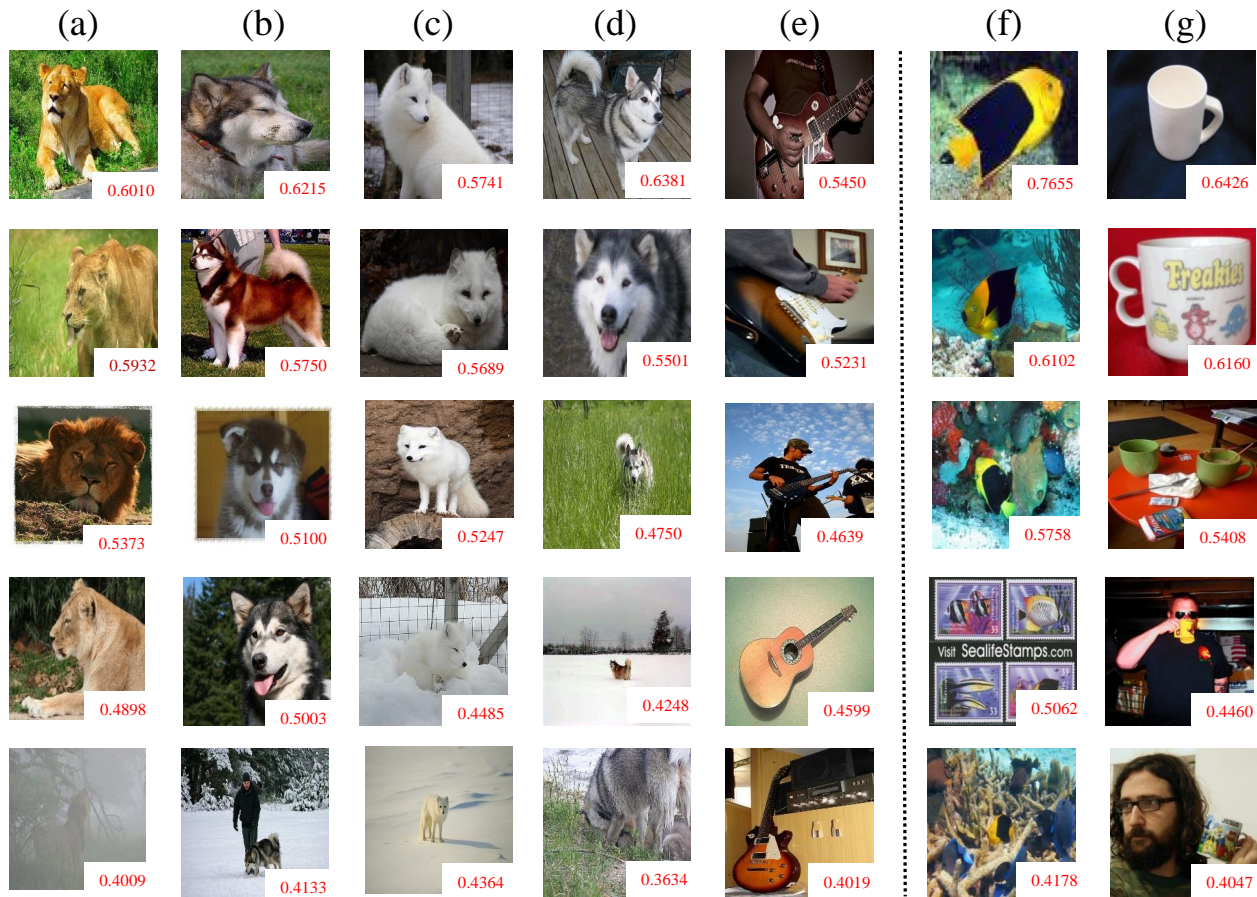


Fig. 6: Visualization of the learned importance: (a), (b), (c), (d) and (e) show support instances sampled from miniImageNet, and each class contains five support instances; (f) and (g) show support instances sampled from tieredImageNet. Each column of support instances is sorted by relative importance.

TABLE VIII: Transductive FSL on miniImageNet and tieredImageNet.

Dataset	Method	1-shot	5-shot
miniImageNet	ICRL-Net	65.55 $\pm$ 0.79	81.87 $\pm$ 0.51
	ICRL-Net+T	67.33 $\pm$ 0.63	82.65 $\pm$ 0.53
tieredImageNet	ICRL-Net	70.56 $\pm$ 0.91	85.62 $\pm$ 0.64
	ICRL-Net+T	72.20 $\pm$ 0.80	86.05 $\pm$ 0.58

### G. Transductive FSL

We further extend the proposed method for transductive FSL by integrating our AIRN with the transductive inference algorithm developed by CAN [47]. Specifically, we firstly utilize the proposed AIRN to obtain the class features and utilize the initial class features to predict the labels of the unlabeled query samples. Then we select several pseudo-labeled unlabeled query samples according to the label confidence criterion proposed by CAN [47]. Finally, the selected pseudo-labeled unlabeled query samples are used together with the initial class features to generate more representative class features. From Table VIII, we can see that performance of the proposed ICRL-Net under the transductive setting (ICRL-Net+T) are further improved.

## V. CONCLUSION

In this paper, we present a novel framework for metric-based FSL by considering the information diversity of instances. The designed instance-adaptive class representation learning network (ICRL-Net) can automatically learn the relative significance of different support instances that belong to the same class. We conducted extensive experiments on four few-shot visual recognition benchmarks, and from the results, we mainly conclude that: 1) exploiting the significance of different instances is critical in obtaining the class-level representation, and the proposed ICRL-Net can adaptively and effectively evaluate the relative significance of different instances; 2) the proposed method outperforms the state-of-the-art FSL counterparts by a large margin, and all the different modules in our ICRL-Net are essential to achieve satisfactory performance. One disadvantage of our method may be that the importance is assessed at the instance level, while the relative importance of the different regions in a visual instance is not considered. How to revaluing the significance of different regions inside one instance remains a potential future work.

## ACKNOWLEDGMENT

The authors would like to thank the handling associate editor and all the anonymous reviewers for their constructive

comments. This research was supported in part by the National Key Research and Development Program of China under No. 2021YFC3300200, the Special Fund of Hubei LuoJia Laboratory under Grant 220100014, and the National Natural Science Foundation of China (Grant No. 62002090 and 62141112).

## REFERENCES

- [1] Kaiming He, Xiangyu Zhang, Shaoqing Ren, and Jian Sun. Deep residual learning for image recognition. In *Proceedings of the IEEE Conference on Computer Vision and Pattern Recognition (CVPR)*, pages 770–778, 2016.
- [2] Gao Huang, Zhuang Liu, Laurens Van Der Maaten, and Kilian Q Weinberger. Densely connected convolutional networks. In *Proceedings of the IEEE Conference on Computer Vision and Pattern Recognition (CVPR)*, pages 4700–4708, 2017.
- [3] Jie Hu, Li Shen, and Gang Sun. Squeeze-and-excitation networks. In *Proceedings of the IEEE Conference on Computer Vision and Pattern Recognition (CVPR)*, pages 7132–7141, 2018.
- [4] Joseph Redmon, Santosh Divvala, Ross Girshick, and Ali Farhadi. You only look once: Unified, real-time object detection. In *Proceedings of the IEEE Conference on Computer Vision and Pattern Recognition (CVPR)*, pages 779–788, 2016.
- [5] Shaoqing Ren, Kaiming He, Ross Girshick, and Jian Sun. Faster r-cnn: Towards real-time object detection with region proposal networks. In *Advances in Neural Information Processing Systems (NeurIPS)*, pages 91–99, 2015.
- [6] Kaiming He, Georgia Gkioxari, Piotr Dollár, and Ross Girshick. Mask r-cnn. In *Proceedings of the IEEE International Conference on Computer Vision (ICCV)*, pages 2961–2969, 2017.
- [7] Li Fe-Fei et al. A bayesian approach to unsupervised one-shot learning of object categories. In *Proceedings Ninth IEEE International Conference on Computer Vision*, pages 1134–1141. IEEE, 2003.
- [8] Li Fei-Fei, Rob Fergus, and Pietro Perona. One-shot learning of object categories. *IEEE Transactions on Pattern Analysis and Machine Intelligence (TPAMI)*, 28(4):594–611, 2006.
- [9] Spyros Gidaris and Nikos Komodakis. Dynamic few-shot visual learning without forgetting. In *Proceedings of the IEEE Conference on Computer Vision and Pattern Recognition (CVPR)*, pages 4367–4375, 2018.
- [10] Hong-Gyu Jung and Seong-Wan Lee. Few-shot learning with geometric constraints. *IEEE Transactions on Neural Networks and Learning Systems*, 31(11):4660–4672, 2020.
- [11] Nan Lai, Meina Kan, Chunrui Han, Xingguang Song, and Shiguang Shan. Learning to learn adaptive classifier–predictor for few-shot learning. *IEEE Transactions on Neural Networks and Learning Systems*, 32(8):3458–3470, 2021.
- [12] Hankook Lee, Sung Ju Hwang, and Jinwoo Shin. Self-supervised label augmentation via input transformations. In *International Conference on Machine Learning (ICML)*, pages 5714–5724, 2020.
- [13] Hainan Li, Renshuai Tao, Jun Li, Haotong Qin, Yifu Ding, Shuo Wang, and Xianglong Liu. Multi-pretext attention network for few-shot learning with self-supervision. In *2021 IEEE International Conference on Multimedia and Expo (ICME)*, pages 1–6. IEEE, 2021.
- [14] Jiang Lu, Sheng Jin, Jian Liang, and Changshui Zhang. Robust few-shot learning for user-provided data. *IEEE Transactions on Neural Networks and Learning Systems*, 32(4):1433–1447, 2021.
- [15] Qinxuan Luo, Lingfeng Wang, Jingguo Lv, Shiming Xiang, and Chunhong Pan. Few-shot learning via feature hallucination with variational inference. In *Proceedings of the IEEE/CVF Winter Conference on Applications of Computer Vision (WACV)*, pages 3963–3972, January 2021.
- [16] Zhizheng Zhang, Cuiling Lan, Wenjun Zeng, Zhibo Chen, and Shih-Fu Chang. Uncertainty-aware few-shot image classification. *IJCAI*, 2021.
- [17] Imtiaz Ziko, Jose Dolz, Eric Granger, and Ismail Ben Ayed. Laplacian regularized few-shot learning. In *International Conference on Machine Learning (ICML)*, pages 11660–11670, 2020.
- [18] Kwonjoon Lee, Subhansu Maji, Avinash Ravichandran, and Stefano Soatto. Meta-learning with differentiable convex optimization. In *Proceedings of the IEEE Conference on Computer Vision and Pattern Recognition (CVPR)*, pages 10657–10665, 2019.
- [19] Jinghang Li and Mengqi Hu. Continuous model adaptation using online meta-learning for smart grid application. *IEEE Transactions on Neural Networks and Learning Systems*, 32(8):3633–3642, 2021.
- [20] Sachin Ravi and Hugo Larochelle. Optimization as a model for few-shot learning. In *International Conference on Learning Representations (ICLR)*, 2017.
- [21] Oriol Vinyals, Charles Blundell, Timothy Lillicrap, Daan Wierstra, et al. Matching networks for one shot learning. In *Advances in Neural Information Processing Systems (NeurIPS)*, pages 3630–3638, 2016.
- [22] Thomas Elsken, Benedikt Staffler, Jan Hendrik Metzen, and Frank Hutter. Meta-learning of neural architectures for few-shot learning. In *Proceedings of the IEEE Conference on Computer Vision and Pattern Recognition (CVPR)*, pages 12365–12375, 2020.
- [23] Chelsea Finn, Pieter Abbeel, and Sergey Levine. Model-agnostic meta-learning for fast adaptation of deep networks. In *International Conference on Machine Learning (ICML)*, page 1126–1135, 2017.
- [24] Andrei A Rusu, Dushyant Rao, Jakub Sygnowski, Oriol Vinyals, Razvan Pascanu, Simon Osindero, and Raia Hadsell. Meta-learning with latent embedding optimization. In *International Conference on Learning Representations (ICLR)*, 2019.
- [25] Qinxuan Luo, Lingfeng Wang, Jingguo Lv, Shiming Xiang, and Chunhong Pan. Few-shot learning via feature hallucination with variational inference. In *Proceedings of the IEEE/CVF Winter Conference on Applications of Computer Vision (WACV)*, pages 3963–3972, 2021.
- [26] Christian Simon, Piotr Koniusz, Richard Nock, and Mehrtash Harandi. Adaptive subspaces for few-shot learning. In *Proceedings of the IEEE Conference on Computer Vision and Pattern Recognition (CVPR)*, 2020.
- [27] Yonglong Tian, Yue Wang, Dilip Krishnan, Joshua B Tenenbaum, and Phillip Isola. Rethinking few-shot image classification: a good embedding is all you need? *arXiv preprint arXiv:2003.11539*, 2020.
- [28] Yinbo Chen, Zhuang Liu, Huijuan Xu, Trevor Darrell, and Xiaolong Wang. Meta-baseline: Exploring simple meta-learning for few-shot learning. In *Proceedings of the IEEE International Conference on Computer Vision (ICCV)*, 2021.
- [29] Jake Snell, Kevin Swersky, and Richard Zemel. Prototypical networks for few-shot learning. In *Advances in Neural Information Processing Systems (NeurIPS)*, pages 4077–4087, 2017.
- [30] Flood Sung, Yongxin Yang, Li Zhang, Tao Xiang, Philip HS Torr, and Timothy M Hospedales. Learning to compare: Relation network for few-shot learning. In *Proceedings of the IEEE Conference on Computer Vision and Pattern Recognition (CVPR)*, pages 1199–1208, 2018.
- [31] Mengye Ren, Eleni Triantafillou, Sachin Ravi, Jake Snell, Kevin Swersky, Joshua B Tenenbaum, Hugo Larochelle, and Richard S Zemel. Meta-learning for semi-supervised few-shot classification. In *International Conference on Learning Representations (ICLR)*, 2018.
- [32] Luca Bertinetto, Joao F Henriques, Philip HS Torr, and Andrea Vedaldi. Meta-learning with differentiable closed-form solvers. In *International Conference on Learning Representations (ICLR)*, 2019.
- [33] Boris Oreshkin, Pau Rodríguez López, and Alexandre Lacoste. Tadam: Task dependent adaptive metric for improved few-shot learning. In *Advances in Neural Information Processing Systems (NeurIPS)*, pages 721–731, 2018.
- [34] Spyros Gidaris and Nikos Komodakis. Generating classification weights with gnn denoising autoencoders for few-shot learning. In *Proceedings of the IEEE Conference on Computer Vision and Pattern Recognition (CVPR)*, pages 21–30, 2019.
- [35] Nikolaos Passalis, Alexandros Iosifidis, Moncef Gabbouj, and Anastasios Tefas. Hypersphere-based weight imprinting for few-shot learning on embedded devices. *IEEE Transactions on Neural Networks and Learning Systems*, 32(2):925–930, 2021.
- [36] Zhengyu Chen, Jixie Ge, Heshen Zhan, Siteng Huang, and Donglin Wang. Pareto self-supervised training for few-shot learning. In *Proceedings of the IEEE Conference on Computer Vision and Pattern Recognition (CVPR)*, pages 13663–13672, 2021.
- [37] Yiluan Guo and Ngai-Man Cheung. Attentive weights generation for few shot learning via information maximization. In *Proceedings of the IEEE Conference on Computer Vision and Pattern Recognition (CVPR)*, pages 13499–13508, 2020.
- [38] Kai Li, Yulun Zhang, Kumpeng Li, and Yun Fu. Adversarial feature hallucination networks for few-shot learning. In *Proceedings of the IEEE Conference on Computer Vision and Pattern Recognition (CVPR)*, pages 13470–13479, 2020.
- [39] Bowen Wang, Liangzhi Li, Manisha Verma, Yuta Nakashima, Ryo Kawasaki, and Hajime Nagahara. Mtunet: Few-shot image classification with visual explanations. In *Proceedings of the IEEE Conference on Computer Vision and Pattern Recognition (CVPR)*, pages 2294–2298, 2021.

- [40] Zhenguo Li, Fengwei Zhou, Fei Chen, and Hang Li. Meta-sgd: Learning to learn quickly for few-shot learning. *arXiv preprint arXiv:1707.09835*, 2017.
- [41] Nikhil Mishra, Mostafa Rohaninejad, Xi Chen, and Pieter Abbeel. A simple neural attentive meta-learner. In *International Conference on Learning Representations (ICLR)*, 2018.
- [42] Qianru Sun, Yaoyao Liu, Tat-Seng Chua, and Bernt Schiele. Meta-transfer learning for few-shot learning. In *Proceedings of the IEEE Conference on Computer Vision and Pattern Recognition (CVPR)*, pages 403–412, 2019.
- [43] Bharath Hariharan and Ross Girshick. Low-shot visual recognition by shrinking and hallucinating features. In *Proceedings of the IEEE International Conference on Computer Vision (ICCV)*, pages 3018–3027, 2017.
- [44] Gregory Koch, Richard Zemel, and Ruslan Salakhutdinov. Siamese neural networks for one-shot image recognition. In *ICML deep learning workshop*, volume 2. Lille, 2015.
- [45] Wenbin Li, Lei Wang, Jinglin Xu, Jing Huo, Yang Gao, and Jiebo Luo. Revisiting local descriptor based image-to-class measure for few-shot learning. In *Proceedings of the IEEE Conference on Computer Vision and Pattern Recognition (CVPR)*, pages 7260–7268, 2019.
- [46] Hang Qi, Matthew Brown, and David G. Lowe. Low-shot learning with imprinted weights. In *Proceedings of the IEEE Conference on Computer Vision and Pattern Recognition (CVPR)*, 2017.
- [47] Ruibing Hou, Hong Chang, Bingpeng Ma, Shiguang Shan, and Xilin Chen. Cross attention network for few-shot classification. In *Advances in Neural Information Processing Systems (NeurIPS)*, pages 4005–4016, 2019.
- [48] Han-Jia Ye, Hexiang Hu, De-Chuan Zhan, and Fei Sha. Few-shot learning via embedding adaptation with set-to-set functions. In *Proceedings of the IEEE Conference on Computer Vision and Pattern Recognition (CVPR)*, pages 8808–8817, 2020.
- [49] Seong Min Kye, Hae Beom Lee, Hoirin Kim, and Sung Ju Hwang. Meta-learned confidence for few-shot learning. *arXiv preprint arXiv:2002.12017*, 2020.
- [50] Yang Zhao, Chunyuan Li, Ping Yu, and Changyou Chen. Remp: Rectified metric propagation for few-shot learning. In *Proceedings of the IEEE Conference on Computer Vision and Pattern Recognition (CVPR) Workshops*, pages 2581–2590, 2021.
- [51] Yikai Wang, Chengming Xu, Chen Liu, Li Zhang, and Yanwei Fu. Instance credibility inference for few-shot learning. In *Proceedings of the IEEE Conference on Computer Vision and Pattern Recognition (CVPR)*, pages 12836–12845, 2020.
- [52] Yikai Wang, Li Zhang, Yuan Yao, and Yanwei Fu. How to trust unlabeled data instance credibility inference for few-shot learning. *IEEE Transactions on Pattern Analysis and Machine Intelligence*, 2021.
- [53] Xiaolong Wang, Ross Girshick, Abhinav Gupta, and Kaiming He. Non-local neural networks. In *Proceedings of the IEEE Conference on Computer Vision and Pattern Recognition (CVPR)*, June 2018.
- [54] Sanghyun Woo, Jongchan Park, Joon-Young Lee, and In So Kweon. Cbam: Convolutional block attention module. In *Proceedings of the European Conference on Computer Vision (ECCV)*, pages 3–19, 2018.
- [55] Petar Veličković, Guillem Cucurull, Arantxa Casanova, Adriana Romero, Pietro Lio, and Yoshua Bengio. Graph attention networks. *arXiv preprint arXiv:1710.10903*, 2017.
- [56] Kai Han, An Xiao, Enhua Wu, Jianyuan Guo, Chunjing Xu, and Yunhe Wang. Transformer in transformer. *arXiv preprint arXiv:2103.00112*, 2021.
- [57] Ashish Vaswani, Noam Shazeer, Niki Parmar, Jakob Uszkoreit, Llion Jones, Aidan N Gomez, Łukasz Kaiser, and Illia Polosukhin. Attention is all you need. In *Advances in Neural Information Processing Systems (NeurIPS)*, pages 5998–6008, 2017.
- [58] Peng Wang, Lingqiao Liu, Chunhua Shen, Zi Huang, Anton van den Hengel, and Heng Tao Shen. Multi-attention network for one shot learning. In *Proceedings of the IEEE Conference on Computer Vision and Pattern Recognition (CVPR)*, July 2017.
- [59] Weijian Xu, Huaijin Wang, Zhuowen Tu, et al. Attentional constellation nets for few-shot learning. In *International Conference on Learning Representations (ICLR)*, 2021.
- [60] Catalin Ionescu, Orestis Vantzos, and Cristian Sminchisescu. Matrix backpropagation for deep networks with structured layers. In *Proceedings of the IEEE International Conference on Computer Vision (ICCV)*, pages 2965–2973, 2015.
- [61] Jin-Hwa Kim, Kyoung-Woon On, Woosang Lim, Jeonghee Kim, Jung-Woo Ha, and Byoung-Tak Zhang. Hadamard product for low-rank bilinear pooling. *arXiv preprint arXiv:1610.04325*, 2016.
- [62] Tsung-Yu Lin, Aruni RoyChowdhury, and Subhransu Maji. Bilinear cnn models for fine-grained visual recognition. In *Proceedings of the IEEE International Conference on Computer Vision (ICCV)*, pages 1449–1457, 2015.
- [63] Min Lin, Qiang Chen, and Shuicheng Yan. Network in network. *arXiv preprint arXiv:1312.4400*, 2013.
- [64] Hongguang Zhang and Piotr Koniusz. Power normalizing second-order similarity network for few-shot learning. In *2019 IEEE winter conference on applications of computer vision (WACV)*, pages 1185–1193. IEEE, 2019.
- [65] Hongguang Zhang, Jing Zhang, and Piotr Koniusz. Few-shot learning via saliency-guided hallucination of samples. In *Proceedings of the IEEE Conference on Computer Vision and Pattern Recognition (CVPR)*, pages 2770–2779, 2019.
- [66] Hongguang Zhang, Philip HS Torr, and Piotr Koniusz. Few-shot learning with multi-scale self-supervision. *arXiv preprint arXiv:2001.01600*, 2020.
- [67] Davis Wertheimer and Bharath Hariharan. Few-shot learning with localization in realistic settings. In *Proceedings of the IEEE Conference on Computer Vision and Pattern Recognition (CVPR)*, pages 6558–6567, 2019.
- [68] Piotr Koniusz and Hongguang Zhang. Power normalizations in fine-grained image, few-shot image and graph classification. *IEEE Transactions on Pattern Analysis and Machine Intelligence*, 2021.
- [69] Micah Goldblum, Steven Reich, Liam Fowl, Renkun Ni, Valeria Cherepanova, and Tom Goldstein. Unraveling meta-learning: Understanding feature representations for few-shot tasks. In *International Conference on Machine Learning (ICML)*, pages 3607–3616. PMLR, 2020.
- [70] Olga Russakovsky, Jia Deng, Hao Su, Jonathan Krause, Sanjeev Satheesh, Sean Ma, Zhiheng Huang, Andrej Karpathy, Aditya Khosla, Michael Bernstein, et al. Imagenet large scale visual recognition challenge. *International journal of computer vision*, 115(3):211–252, 2015.
- [71] Alex Krizhevsky, Vinod Nair, and Geoffrey Hinton. Cifar-100 (canadian institute for advanced research). URL <http://www.cs.toronto.edu/kriz/cifar.html>.
- [72] Debasmit Das and C. S. George Lee. A two-stage approach to few-shot learning for image recognition. *IEEE Transactions on Image Processing*, 29:3336–3350, 2020.
- [73] Chi Zhang, Yujun Cai, Guosheng Lin, and Chunhua Shen. Deepemd: Few-shot image classification with differentiable earth mover’s distance and structured classifiers. In *Proceedings of the IEEE Conference on Computer Vision and Pattern Recognition (CVPR)*, pages 12203–12213, 2020.
- [74] Jaekyeom Kim, Hyoungseok Kim, and Gunhee Kim. Model-agnostic boundary-adversarial sampling for test-time generalization in few-shot learning. In *Proceedings of the European Conference on Computer Vision (ECCV)*, 2020.
- [75] Wei-Yu Chen, Yen-Cheng Liu, Zsolt Kira, Yu-Chiang Frank Wang, and Jia-Bin Huang. A closer look at few-shot classification. *arXiv preprint arXiv:1904.04232*, 2019.



**Mengya Han** received the B.S. degree in Computer Science from the Bengbu University, Bengbu, China, and the M.S degree in the School of Computer Science and Information Engineering, Hefei University of Technology, Hefei, China. She is currently a PhD student in the School of Computer Science, Wuhan University, China. Her research interests are primarily in computer vision and machine learning.



**Yibing Zhan** received a B.E. and a Ph.D. from the University of Science and Technology of China in 2012 and 2018, respectively. From 2018 to 2020, he was an Associate Researcher in the Computer and Software School at the Hangzhou Dianzi University. He is currently an algorithm scientist at the JD Explore Academy. His research interest is in graphical models and multimodal learning, including cross-modal retrieval, scene graph generation, and graph neural networks. He has publications on various top conferences and journals, such as CVPR, ACM MM,

AAAI, IJCV, and IEEE TMM.



**Yong Luo** received the B.E. degree in Computer Science from the Northwestern Polytechnical University, Xi'an, China, and the D.Sc. degree in the School of Electronics Engineering and Computer Science, Peking University, Beijing, China. He is currently a Professor with the School of Computer Science, Wuhan University, China. His research interests are primarily on machine learning and data mining with applications to visual information understanding and analysis. He has authored or co-authored over 60

papers in top journals and prestigious conferences including IEEE T-PAMI, IEEE T-NNLS, IEEE T-IP, IEEE T-KDE, IEEE T-MM, ICCV, WWW, IJCAI and AAAI. He is serving on editorial board for IEEE T-MM. He received the IEEE Globecom 2016 Best Paper Award, and was nominated as the IJCAI 2017 Distinguished Best Paper Award. He is also a co-recipient of the IEEE ICME 2019 and IEEE VCIP 2019 Best Paper Awards.



**Bo Du** received the PhD degree from the State Key Laboratory of Information Engineering in Surveying, Mapping and Remote Sensing, Wuhan University, Wuhan, China, in 2010. He is currently a professor with the School of Computer, Wuhan University. He has published more than 100 scientific papers, such as the IEEE Transactions on Geoscience and Remote Sensing, IEEE Transactions on Neural Networks and Learning Systems, IEEE Transactions on Image Processing, IEEE Transactions on Cybernetics, AAAI, and IJCAI. His research interests include pattern

recognition, hyperspectral image processing, and signal processing.



**Han Hu** received the B.E. and Ph.D. degrees from the University of Science and Technology of China, China, in 2007 and 2012, respectively. He is currently a Professor with the School of Information and Electronics, Beijing Institute of Technology, China. His research interests include multimedia networking, edge intelligence, and space-air-ground integrated network. He received several academic awards, including the Best Paper Award of the IEEE TCSVT 2019, the Best Paper Award of the IEEE Multimedia Magazine 2015, and the Best Paper

Award of the IEEE Globecom 2013. He has served as an Associate Editor of IEEE TMM and Ad Hoc Networks, and a TPC member of Infocom, ACM MM, AAAI, and IJCAI.



**Yonggang Wen** (M'08-S'14-F'20) is the Professor of Computer Science and Engineering at Nanyang Technological University (NTU), Singapore. He has also served as the Associate Dean (Research) at College of Engineering at NTU Singapore since 2018. He served as the Acting Director of Nanyang Technopreneurship Centre (NTC) at NTU from 2017 to 2019, and the Assistant Chair (Innovation) of School of Computer Science and Engineering (SCSE) at NTU from 2016 to 2018. He received his PhD degree in Electrical Engineering and Com-

puter Science (minor in Western Literature) from Massachusetts Institute of Technology (MIT), Cambridge, USA, in 2008. He is a co-recipient of multiple journal best papers awards, including IEEE Transactions on Circuits and Systems for Video Technology (2019), IEEE Multimedia (2015), and several best paper awards from international conferences, including 2020 IEEE VCIP, 2016 IEEE Globecom, 2016 IEEE Infocom MuSIC Workshop, 2015 EAI/ICST Chinacom, 2014 IEEE WCSP, 2013 IEEE Globecom and 2012 IEEE EUC. He received 2016 IEEE ComSoc MMTC Distinguished Leadership Award. His research interests include cloud computing, green data center, distributed machine learning, blockchain, big data analytics, multimedia network and mobile computing. He is a Fellow of IEEE.



**Dacheng Tao** (F'15) is currently an Advisor and a Chief Scientist of the Digital Science Institute, Faculty of Engineering, University of Sydney, Darlington, NSW, Australia. He is also the Director of the JD Explore Academy and a Vice President of JD.com. He mainly applies statistics and mathematics to artificial intelligence and data science, and his research is detailed in one monograph and over 200 publications in prestigious journals and proceedings at leading conferences. Dr. Tao received the 2015 Australian ScopusEureka Prize, the 2018 IEEE ICDM Research Contributions Award, and the 2021 IEEE Computer Society McCluskey Technical Achievement Award. He is a Fellow of the Australian Academy of Science, AAAS, and ACM.